

# EFFICIENT MODELING OF TIME-DEPENDENT HOT-ELECTRON-INDUCED MOSFET DEGRADATION WITH A HYDRODYNAMIC-BOLTZMANN TRANSPORT EQUATION HYBRID METHOD

Shiuh-Luen Wang and Neil Goldsman  
*Electrical Engineering Department*  
*University of Maryland*  
*College Park, MD 20742*

## Abstract

An easily implemented method, which combines physical rigor and engineering practicality, for predicting hot-electron-induced, time-dependent, device reliability problems is presented. In this work we focus mainly on predicting gate-leakage currents and the degradation of current-voltage characteristics (I-V) in MOSFET's. The presented method is based on a Hydrodynamic-Boltzmann transport equation model, which provides the distribution function over a device. Results agree well with both experiment and costly Monte Carlo calculations, while requiring much less the CPU time to calculate.

## I. INTRODUCTION

Accurate modeling of many hot-electron effects in semiconductor devices requires knowledge of the energy distribution function. However, models previously proposed, including the popular Richardson's equation method, are often based on the incorrect assumption that the distribution function is Maxwellian. Other methods are physically accurate, but often require too much CPU time. Recently a new approach which combines the hydrodynamic transport model with the homogeneous-field Boltzmann transport equation to extrapolate the distribution function has been developed [1]. This method includes physical rigor but obviates the need for a great deal of computation time. In this work, we apply this hydrodynamic-Boltzmann transport equation model to investigate the hot-electron-induced degradation in MOSFET's. Once the distribution function and average energy has been obtained from this model, we use the information to predict MOSFET gate-leakage current, oxide-charge deposition, interface-trap generation, and device I-V characteristics as a function of stressing time. Excellent agreement with experiment is attained; calculations have also been shown to agree with Monte Carlo simulations, while requiring less than 1/1000 the CPU time to evaluate.

## II. MODEL DESCRIPTIONS

### II.1. Hydrodynamic-Boltzmann Transport Equation Model

The Hydrodynamic-Boltzmann transport equation model for electrons consists of five equations: the energy balance equation (1), and the homogeneous-field Boltzmann transport equation (2), as well as the Poisson, continuity and momentum balance equations. The first two equations are given below. The energy balance equation along with the Poisson, continuity and moment balance equations form the well-known hydrodynamic transport model. The homogeneous-field Boltzmann equation is obtained by replacing the drift and diffusion terms of the Boltzmann equation with a single *effective-electric field* term.

$$\vec{v} \cdot \nabla w = -e(\vec{v} \cdot \vec{E}) - \frac{2}{3n} \nabla \cdot (n\vec{v}w) - \frac{1}{n} \nabla \cdot \vec{Q} - \frac{w - w_0}{\tau_w(w)} \quad (1)$$

$$-\frac{e}{h} \vec{E}_{ef}(\vec{r}) \cdot \nabla_{\vec{k}} f(\vec{r}, \vec{k}) = \left( \frac{\partial f(\vec{r}, \vec{k})}{\partial t} \right)_{ac} + \left( \frac{\partial f(\vec{r}, \vec{k})}{\partial t} \right)_{iv} + \left( \frac{\partial f(\vec{r}, \vec{k})}{\partial t} \right)_{ii} \quad (2)$$

where  $\vec{v}$  is the electron drift velocity,  $w$  is the electron average energy,  $\vec{E}$  is the actual electric field,  $n$  is the electron concentration,  $\vec{Q}$  is the heat flow vector,  $\tau_w$  is the energy relaxation time,  $\vec{E}_{ef}$  is the effective-electric field,  $\vec{r}$  is the electron instantaneous position,  $\vec{k}$  is the electron wave vector,  $f(\vec{r}, \vec{k})$  is the electron momentum distribution function, and the subscripts *ac*, *iv*, *ii* correspond to acoustic phonons, intervalley phonons, and impact ionization respectively.

This model has been described in [1]. Briefly, the general approach is first to obtain the electric field, carrier concentration, drift velocity, and average electron energy from a solution to the hydrodynamic transport equations. From these average values, an *effective-electric field* profile is obtained. The homogeneous-field Boltzmann equation (2) is then solved at each spatial coordinate using the corresponding *effective-electric field* as input to obtain the electron distribution function throughout the device. By having to solve only the hydrodynamic transport equations and the homogeneous-field Boltzmann equation independently, as opposed to the full Boltzmann equation, this model provides a computationally economical scheme for ascertaining nonlocal effects and the distribution function.

In this work, MOSFET degradation is predicted from the results obtained by implementing the aforementioned model. To facilitate investigating time-dependent reliability problems, the initial values (time  $t=0$ ) for electrostatic potential and carrier concentrations are provided by a 2-D Poisson-continuity equation solver. With concentration and potential as input, the energy balance equation (1) is solved for average electron energy in two dimensions using a new globally convergent method [2]. To evaluate the hydrodynamic-Boltzmann transport equation model, we also need to solve the homogeneous-field Boltzmann equation (2) as indicated above. Here this equation is solved with the transport model given by [3], while closely following the procedures in [4]. We first formulate the equation in terms of the following third order Legendre series, while accounting for the effects of acoustic and intervalley phonon scattering, impact ionization, as well as silicon's nonparabolic, ellipsoidal band structure. The formulated Boltzmann equation is then solved numerically using sparse matrix algebra.

$$f(\vec{k}) = f_0(\varepsilon) + k f_1(\varepsilon) P_1(\cos\theta) + k^2 f_2(\varepsilon) P_2(\cos\theta) \quad (3)$$

where  $\theta$  is the angle between  $\vec{E}_{ef}$  and  $\vec{k}$ ,  $P_1(\cos\theta) = \cos\theta$ ,  $P_2(\cos\theta) = \frac{3}{2}\cos^2\theta - \frac{1}{2}$ , and  $f_0(\varepsilon)$ ,  $k f_1(\varepsilon)$ , and  $k^2 f_2(\varepsilon)$  are the coefficients of the three Legendre polynomials respectively.

## II.2. Gate-Leakage Current

We use a Richardson-like equation for thermal emission over the oxide barrier [5]. Unlike Richardson's equation which is based on a Maxwellian, the new expression is derived from the physics-based hot-electron distribution function, which is found from the model described above.

$$J_g(\vec{r}) = \frac{2\pi en(\vec{r})}{3h^3} (m_t^2 m_l)^{1/2} \left[ \frac{2}{m_t^{1/2}} + \frac{1}{m_l^{1/2}} \right] \int_{\Phi_B}^{\infty} f(\vec{r}, \varepsilon) \gamma(\varepsilon) d\varepsilon \quad (4)$$

where  $m_t$  and  $m_l$  are silicon's transverse and longitudinal effective masses respectively,  $\gamma(\varepsilon)$  is silicon's nonparabolic dispersion relation [3],  $\Phi_B$  is the oxide barrier height.  $f(\vec{r}, \varepsilon)$  is the energy distribution function. The effects of Schottky barrier lowering and electron tunneling are accounted for by adjusting the oxide barrier height [6].

It is worth noting that the oxide field near the drain junction is reversed in direction and tends to repel the emitted electrons back to substrate when the device is operated in saturation region. To account for this effect, a critical-injection angle between the oxide field and the Si/SiO<sub>2</sub> interface is introduced, below which injected electrons do not contribute to the gate current [7].

## II.3. Oxide-Charge and Interface-State Buildup and Device Degradation in Time

We predict time-dependent oxide-charge and interface-state buildup by using the following equations. Equation (5) describes the exponential relationship between the occupation of oxide states, the gate-current density, and the device stressing time [6]. The increase in the interface-state density is given in Eqn. (6) which was proposed in [8].

$$N_{ox}(\vec{r}, t) = \sum_i N_{oxi} \left[ 1 - \exp\left(-\frac{\sigma_i J_g(\vec{r}) t}{e}\right) \right] \quad (5)$$

$$\Delta D_{it}(\vec{r}, t) = D_{it, sat} \frac{\frac{\sigma_{it} J_g(\vec{r}) t}{e}}{1 + \frac{\sigma_{it} J_g(\vec{r}) t}{e}} \quad (6)$$

where  $N_{oxi}$  is the density of type  $i$  oxide traps,  $N_{ox}(\vec{r}, t)$  is the number of oxide states filled at time  $t$ ,  $\sigma_i$  is the cross section of oxide trap  $i$ ,  $D_{it, sat}$  is the saturation value of the interface-state density ( $eV^{-1}cm^{-2}$ ),  $\Delta D_{it}(\vec{r}, t)$  is the increased interface-state density, and  $\sigma_{it}$  is the interface-state generation cross-section.

After device operation, some charge becomes trapped in the oxide and interface-states are generated. This often causes a localized perturbation on the potential and carrier distributions near the drain region of the device. This effect can be easily understood by examining the Poisson equation at time  $t_1$ :

$$\begin{cases} \nabla \cdot \nabla \phi(\vec{r}, t_1) = \frac{eN_{ox}(\vec{r}, t_1)}{\epsilon_{ox}} & \text{SiO}_2 \\ \nabla \cdot \nabla \phi(\vec{r}, t_1) = \frac{e}{\epsilon_s} (n' - p' - N) & \text{Si} \\ \epsilon_s \left. \frac{\partial \phi(\vec{r}, t_1)}{\partial y} \right|_{Si} = \epsilon_{ox} \left. \frac{\partial \phi(\vec{r}, t_1)}{\partial y} \right|_{SiO_2} + Q_{int}(\vec{r}, t_1) & \text{Si/SiO}_2 \end{cases} \quad (7)$$

where  $\phi(\vec{r}, t_1)$  is the new potential because of the perturbation caused by the trapped oxide charges and generated interface states,  $n'$  and  $p'$  are the new electron and hole concentrations,  $N$  is the net fixed charge density,  $Q_{int}(\vec{r}, t_1)$  is the generated interface traps which can be calculated from  $\Delta D_{it}(\vec{r}, t_1)$ .

Here the new potential is determined in two dimensions using the time perturbation method [8]. With this method, the new potential can be decomposed into a time independent part and a time dependent part, i.e. at time  $t_1$ ,

$$\phi(\vec{r}, t_1) = \psi(\vec{r}) + u(\vec{r}, t_1) \quad (8)$$

where  $u(\vec{r}, t_1)$  is the perturbation potential at time  $t_1$ , and  $\psi(\vec{r})$  is the original potential.

We start with a potential distribution and electron concentrations obtained from a DD simulator. Then, the perturbation potential is obtained by substituting relation (8) into (7) and solving the resulting equations. After the perturbation potential is determined, local corrections are made to the carrier concentrations. In time, as more charge becomes trapped in the oxide and more interface states are generated, we periodically use the perturbation method to re-evaluate the Poisson and continuity equations. At each iteration, the new gate current and I-V characteristics are calculated using the updated potential distributions and charge concentrations. The overall calculation scheme is shown in Fig. 1.

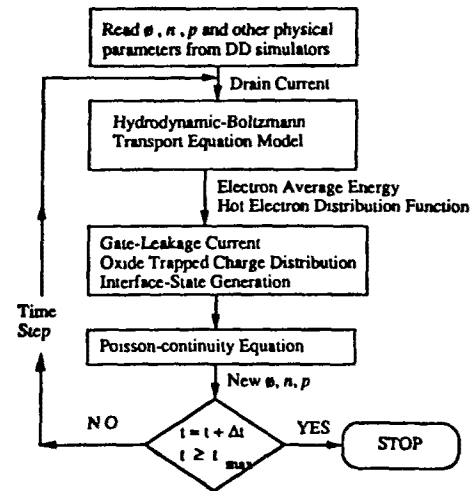


Fig. 1 Hot-electron-induced time-dependent MOSFET degradation prediction scheme based on the hybrid hydrodynamic-Boltzmann transport equation model.

### III. RESULTS

To demonstrate the capabilities of the presented method, we simulated NMOSFET's with channel length  $1.2 \mu m$  and  $0.6 \mu m$  respectively. Excellent agreement of the electron energy distribution functions calculated by our model and the results obtained from Monte Carlo simulations was

attained as shown in Fig. 2. Figure 3 shows the calculated gate currents agree very well with experiment for the  $1.2 \mu\text{m}$  device. Reasonable values for temporal evolution of gate current and drain current for the  $0.6 \mu\text{m}$  device have also been obtained as shown in Figs. 4 and 5.

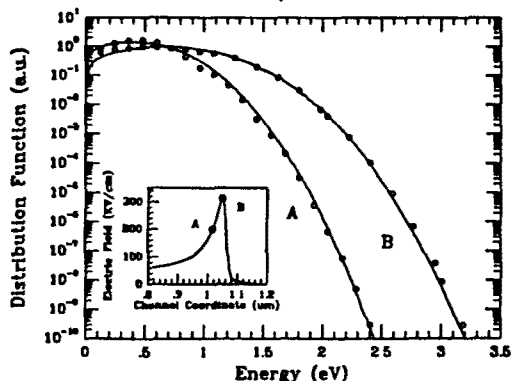


Fig. 2 Comparison of the distribution functions obtained while using the presented model versus Monte Carlo calculations at channel coordinates  $1.02 \mu\text{m}$  (A) and  $1.05 \mu\text{m}$  (B). The device has a gate length of  $1.2 \mu\text{m}$  and is biased at  $V_d = 6.0\text{V}$  and  $V_g = 7.0\text{V}$ . The solid lines were calculated by the presented method. The open circles were calculated by Monte Carlo simulations. The insert shows the lateral electric field along the channel (around the drain junction).

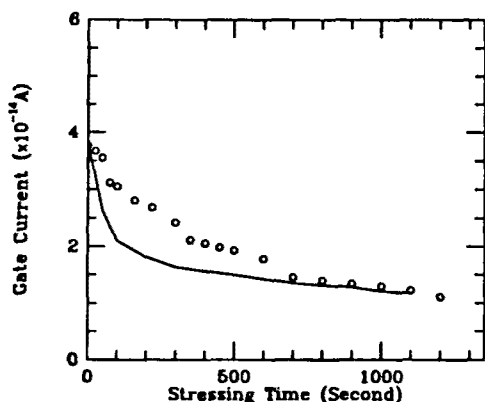


Fig. 4 Measured and calculated gate current versus stressing time. Stress condition is  $V_d = V_g = 4.75\text{V}$ . The open circles were calculated by the presented method; the solid line is from experimental data.  $L/W = 0.6 \mu\text{m}/50 \mu\text{m}$ ,  $T_{ox} = 153 \text{\AA}$ .  $T_{ox} = 153 \text{\AA}$ .

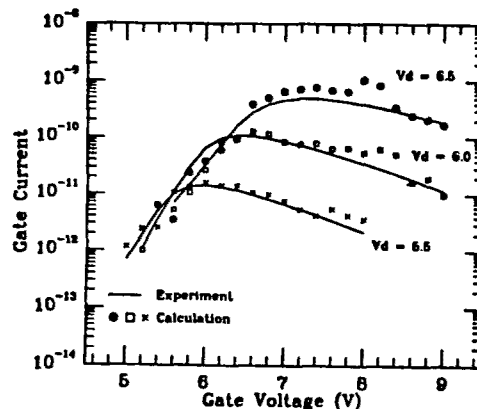


Fig. 3 Gate current versus gate voltage. The points were calculated by the presented method; the solid lines are experimental values.  $L/W = 1.2 \mu\text{m}/50.8 \mu\text{m}$ ,  $T_{ox} = 150 \text{\AA}$ .

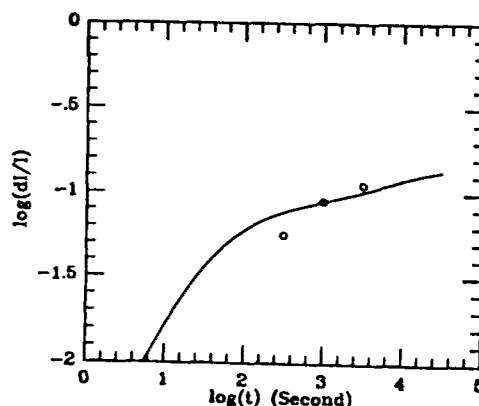


Fig. 5 Calculated drain current degradation as a function of stressing time. Stress condition is  $V_d = 2V_g = 5\text{V}$ . Measurement condition is  $V_d = 0.1\text{V}$  and  $V_g = 2.5\text{V}$ . The solid line was calculated by the presented method; the open circles are experimental values.  $L/W = 0.6 \mu\text{m}/50 \mu\text{m}$ ,  $T_{ox} = 153 \text{\AA}$ .

**Acknowledgements:** The authors are grateful to the National Science Foundation and the Semiconductor Research Corporation for supporting this work.

- [1] S.-L. Wang, N. Goldsman, and K. Hennacy, to appear in IEEE Trans. Electron Devices.
- [2] Q. Lin, N. Goldsman, and G. Tai, Int'l Workshop on Computational Electronics (1992).
- [3] C. Jacoboni and L. Reggiani, Rev. Modern Phys. **55**, 645 (1983).
- [4] S.-L. Wang, N. Goldsman, and K. Hennacy, J. Appl. Phys. **71**, 1815 (1992).
- [5] S.-L. Wang, N. Goldsman, L. Henrickson, and J. Frey, IEDM Tech. Dig. 447 (1990).
- [6] T. H. Ning and H. N. Yu, J. Appl. Phys. **45**, 5373 (1974).
- [7] M. Wada, S. Shibata, M. Konaka, W. Iizaka, and R. Dang, IEDM Tech. Dig. 223 (1981).
- [8] R. Rakkhit, M. Peckerar, and C. T. Yao, Proceedings of the IRPS 103 (1989).